CLASSIFICATION OF AIRCRAFT IMAGES USING DIFFERENT ARCHITECTURES OF RADIAL BASIS FUNCTION NEURAL NETWORK: A PERFORMANCE COMPARISON

Puteh Saad, Subariah Ibrahim and Nur Safawati Mahshos

Department of Software Engineering, Faculty of Computer Science & Information System
University Technology Malaysia, 81310 Skudai, Johor, Malaysia
Tel: +607-5532344 Fax: +607-5565044
Email : puteh@utm.my, subariah@utm.my and shafos04@gmail.com

Abstract ; Four Radial Basis Network architectures are evaluated for their performance in terms of classification accuracy and computation time. The architectures are Radial Basis Neural Network, Goal Oriented Radial Basis Architecture, Generalized Gaussian Network, Probabilistic Neural Network. Zernike Invariant Moment is utilized to extract a set of features from the aircraft image. Each of the architectures is used to classify the image feature vectors. It is found that Generalized Gaussian Neural Network Architecture portrays perfect classification of 100% at a fastest time. Hence, the Generalized Gaussian Neural Network Architecture has a high potential to be adopted to classify images in a real-time environment.

Keywords; Zernike Invariant Moment, Aircraft Image Classification, Radial Basis Neural Network, Generalized Gaussian Network, Probabilistic Neural Network

1. INTRODUCTION

Currently there are numerous types of aircraft invented for a variety of uses namely; cargo for transportation of goods, commercial for transporting passengers and military for national defense. Their shapes and designs vary accordingly. Identification and classification of aircrafts are needed for national security reasons and also for education purposes. For instance, cargo and commercial aircrafts are allowed to tree-pass the country's airborne, however military aircraft are strictly forbidden unless approved by the country's national security department. Production of aircraft progressing rapidly thus only a few aircraft passionate individual can identify them correctly, on the other hand majority cannot fathom the type of aircraft based on their shape.

A few works had been published on this area. Somaie *et al.* (2001) recognized 2-D aircraft images using Back-Propagation(BP) algorithm. They utilized Hotelling Transform to extract a set of features. They used 60 to 500 neurons in the hidden layer. The time taken to train the BP algorithm escalated to 86.5 hours. The recognition performance is 95% as the hidden neuron is

less than 60 or more than 500 neurons at 3.4 seconds to 86.5 hours depending on the number of hidden layer neurons. Abo-Zaid recognized samples of four types of aircraft images represented as 2-D images using Back Propagation Algorithm (Abo-Zaid, 1996). An example of Translation Invariant Transform (TIT) known as MT-Transform was used to obtain a set of invariant features from image samples. He achieved 100 % classification rate, however he do not mentioned the computation time utilized. Botha use BP and achieve 74.07% accuracy with 6 hidden neurons. He, too does not state the computation time taken (Botha, 2004). Chun et al also use BP and achieve 85% accuracy (Chun et al, 2001). He also does not state the computation time taken. On the other hand Fatemi et al uses RBF and achieve 90% accuracy (Fatemi et al, 2003). They too disclosed the computation time utilized to classify the aircraft images.

In our endeavour, Zernike Invariant Moment technique is chosen to extract a set of invariant features from aircraft images due to its accuracy in terms of inter-class variances as reported in (Puteh,2004). The resulting feature vectors are then classified into appropriate class using RBF based architecture. Four different RBF based architectures are evaluated namely; Radial Basis Architecture, Goal Oriented Radial Basis Architecture, Generalized Gaussian Neural Network Architecture and Probabilistic Neural Network Architecture.

The next section of the paper explains ZMI as Feature Extraction technique. Section 3 describes RBF to classify the aircraft image features. The paper continues with Section 4 reporting the implementation. Section 5 discusses the results and Section 6 is the conclusion.

2. ZERNIKE MOMENT INVARIANT

Zernike Moment (Z.M) is chosen since it is invariant to rotation and insensitive to noise. Another advantage of Z.M is the ease of image reconstruction because of its orthogonality property (Teague,1980). Z.M is the projection of the image function onto orthogonal basis functions. Z.M also has a useful rotation invariance property where the magnitude of Z.M will not change for a rotated image. Another main property of Z.M is the ease of image reconstruction because of its orthogonality property. The major drawback of Z.M is it's computational complexity (Mukundan,1998). This is due to the recursive computation of Radial Polynomials. However in this study, we overcome the problem of computational complexity by adopting a non recursive computation of Radial Polynomials. The computation is based on the relationship between Geometric Moment Invariant and Z.M in order to derive Zernike Invariant Moment.

The Z.M of order p with repetition q for a continuos image function $f(x,y)$
that vanishes outside the unit circle is as shown in Equation. 1.1.

$$Z_{pq} = \frac{p+1}{\pi} \iint_{x^2+y^2=1} f(r,\theta) V^*_{pq} r dr d\theta \qquad (1.1)$$

To compute a Z.M of a given image, the center of the image is taken as the origin and pixel coordinates are mapped to the range of unit circle, i.e. $x^2 + y^2 = 1$. The functions of V_{pq} (r, θ) denote Zernike Polynomials of order p with repetition q, and * denotes a complex conjugate where the Zernike Polynomials are defined as functions of the polar coordinates r, θ. Equations relating Zernike and Geometric Moment up to third order are given below

Thus $|Z_{pq}|$, the magnitude of the Z.M, can be taken as a rotation invariant feature of the underlying image function. Rotation invariants and their corresponding expressions in Geometric Moment are given below until the order of three:

$$\left.\begin{aligned} Z_{00} &= (1/\pi)\, M_{00} \\ |Z_{11}|^2 &= (2/\pi)^2 (M_{10}^2 + M_{01}^2) \\ Z_{20} &= (3/\pi)[2M_{20} + M_{02}) - M_{00}] \\ |Z_{22}|^2 &= (3/\pi)^2 [(M_{20} - M_{02})^2 + 4 M_{11}^2) \\ |Z_{31}|^2 &= (12/\pi)^2 [(M_{30} + M_{12})^2 + (M_{03} + M_{21})^2] \\ |Z_{33}|^2 &= (4/\pi)^2 [(M_{30} - 3M_{12})^2 + (M_{03} - 3M_{21})^2] \end{aligned}\right\} \qquad (1.2)$$

3. RADIAL BASIS NEURAL NETWORK

Radial Basis Neural Network or RBF consists of three layers of neurons; input, hidden and output. Neurons in the input layer represent a set of input data. The hidden neurons transform input nodes non-linearly into a high-dimension space using radial basis function. The hidden layer is also known as the radial basis layer. The output from the hidden neurons is then transformed linearly to output neuron. The justification behind this is that according to Cover (1965), a pattern-classification problem that is transformed into a high-dimension space has a probability to be linearly separable than in a low-dimensional space (Haykin, 1994). Theoretically, the more neurons in the hidden layer, the more accurate will be the classification.

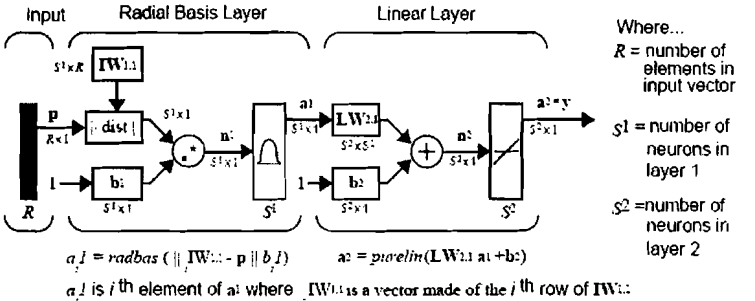

Figure 1: Structure of RBF neural network

In this study four different RBF architectures are explored. In the Radial Basis Architecture shown in Figure 2, the number of hidden nodes is equivalent to input data in the training data. In the Goal-Oriented Radial Basis Architecture as depicted in Figure 3, the number of nodes is added progressively until a desired outcome is produced. The Generalized Gaussian Network Architecture as in Figure 4 consists of a set of hidden units centered at every training data. This unit is known as "kernels" that represent probability density functions normally of type Gaussians. The Generalized Gaussian Network Architecture is often used for function approximations for smooth functions, so it should be able to solve any smooth function approximation problem given enough data. Figure 5 illustrates The Probabilistic Neural Network Architecture. It has a competitive layer after the linear output layer that classifies data based on the RBF unit with the largest output (Demuth and Beale, 2001).

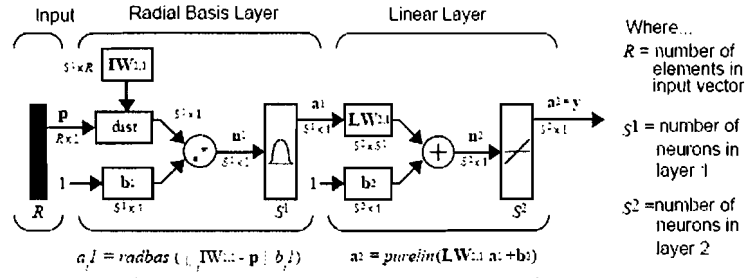

Figure 2 : Radial Basis Architecture

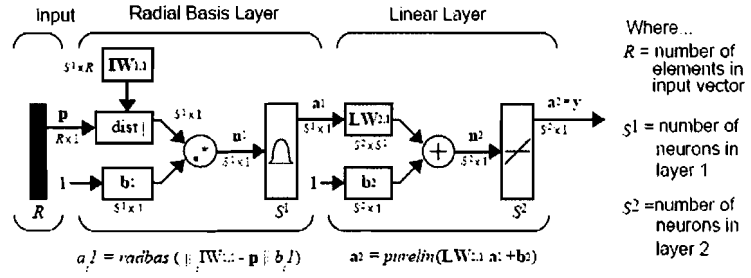

Figure 3: Goal-Oriented Radial Basis Architecture

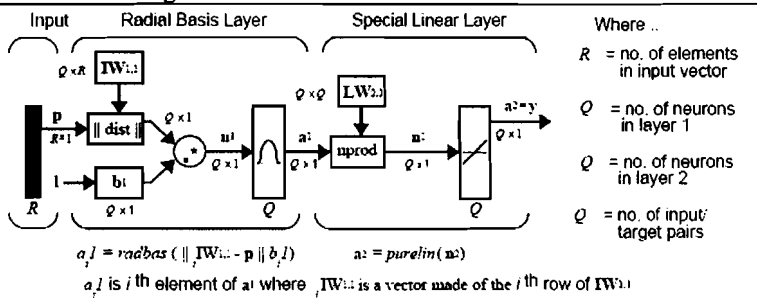

Figure 4: Generalized Gaussian Neural Network

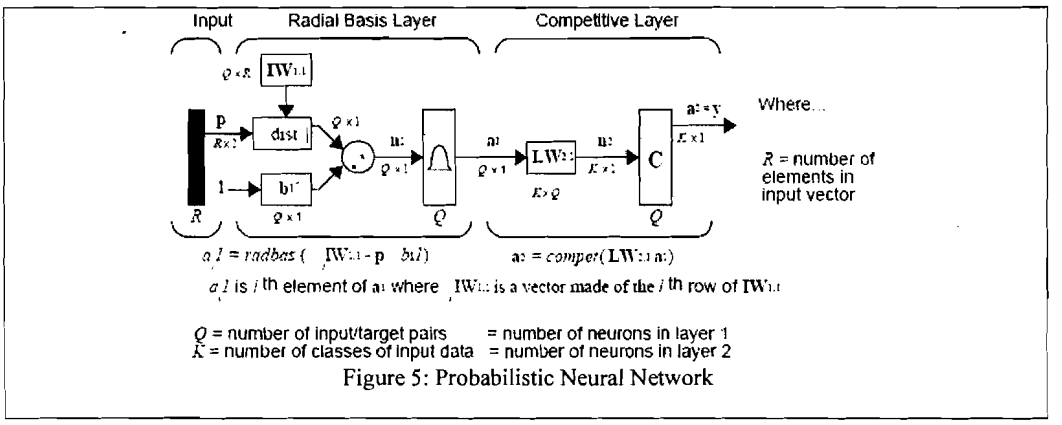

Figure 5: Probabilistic Neural Network

4. CROSS VALIDATION

A *k*-fold cross validation technique is chosen to validate the classification results. Here image samples are divided into *k* subset. Then, cross validation process repeat *k* times to make sure all the subsets were trained and tested. The number of correct classification is computed using equation (5.7). *n* is refers to the number data test. If testing vector is true, $\sigma(x,y)t=1$. However, if testing vector is wrong, then $\sigma(x,y)t=0$. The percentage of correct classification is given by (5.8).

$$PCC_k = 100\frac{1}{G}\sum_{k=1}^{4} NCC_k \qquad (5.7)$$

$$NCC_k = \sum_{t=1}^{n} \sigma(x,y)_t \qquad (5.8)$$

5. IMPLEMENTATION, RESULTS AND DISCUSSION IMAGE ACQUISITION AND PREPROCESSING

The coloured aircraft images that are downloaded from internet (www.airliners.net) are converted into gray-level format. Noise is then removed from the image and subsequently it is thresholded using Otsu thresholding algorithm. The resulting image is then saved using the *.raw* format. Before the image file is closed, its width and height in pixels are noted since the dimensions will become an input to the feature extraction phase. The aircraft image samples are grouped into three categories based on their types. Category 1 represents commercial aircraft. Category 2 represents cargo and finally Category 3 represents military. Figure 6, 7 and 8 show the original images of each category of aircraft.

In this study, each aircraft image will become 13 images as depicted in Figure 9. For each aircraft there are 12 images perturbed by scaling and rotation factors. The purpose of this process is to test the invariant properties and the robustness of the feature extraction techniques adopted. Basically, there are 4 different of scaling factors chosen namely 0.5, 0.75, 1.3 and 1.5. For rotation factors, angles of 5°, 15°, 45° and 90° was chosen. While four images for each aircraft are perturbed by both factors (0.5 with 5°, 0.75 with 15°, 1.3 with 45° and 1.5 with 90°). Each category of aircraft has 10 different type of model. Hence each category consists of 10 original images and 120 perturbed images thus making a total of 390 images.

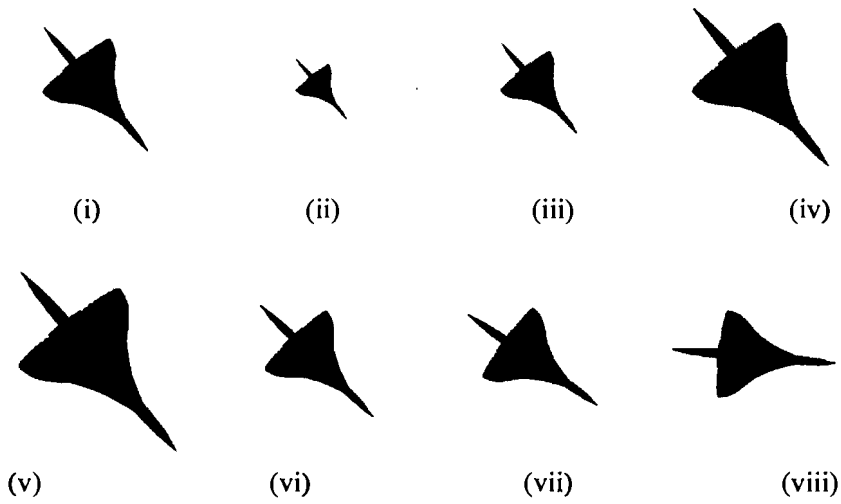

Figure 9 : Image (a) with its variations

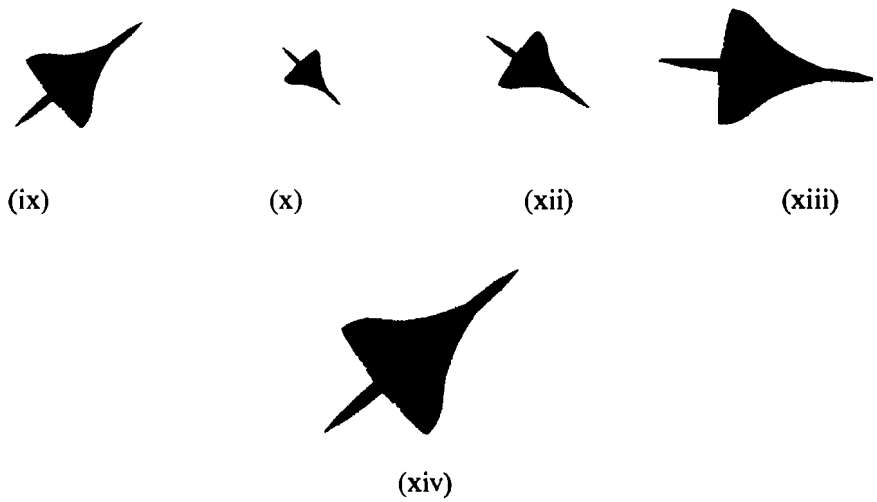

Figure 9 : Image (a) with its variations (cont'.)

Table 4 : Type of variations of aircraft images

Image	Variation
(i)	Original image
(ii)	the image is reduced to half of its original size
(iii)	the image is reduced to 0.7 of its original size
(iv)	the image is enlarged 1.3 its original size
(v)	the image is enlarged 1.3 its original size
(vi)	the image is rotated to 5°
(vii)	the image is rotated to 15°
(viii)	the image is rotated to 45°
(ix)	the image is rotated to 90°
(x)	the image is reduced to 0.5 and rotated to 5°
(xi)	the image is reduced to 0.75 and rotated to 15°
(xii)	the image is enlarged 1.3 and rotated to 45°
(xiii)	the image is enlarged 1.5 and rotated to 90°

Feature Extraction

Zernike Moment features are extracted from image samples using equation (1.2). Table 5 depicts the Z.M features vectors of the same image.

Table 5 : The Z.M Feature Vector of Image (a) and its Variants

ZMI	1	2	3	4	5	6
Original	0.00000	0.00000	0.496054	0.008847	0.020535	0.009627
5°	0.00000	0.00000	0.495574	0.008694	0.019817	0.008370
15°	0.00000	0.00000	0.495431	0.008739	0.020038	0.009627
45°	0.00000	0.00000	0.497110	0.009031	0.020004	0.007078
90°	0.00000	0.00000	0.495590	0.008648	0.020367	0.006955
0.5	0.00000	0.00000	0.495738	0.008825	0.020038	0.009411
0.75	0.00000	0.00000	0.495770	0.008757	0.019979	0.009484
1.3	0.00000	0.00000	0.495620	0.008701	0.020155	0.009549
1.5	0.00000	0.00000	0.495642	0.008691	0.020191	0.009568
15° x 0.75	0.00000	0.00000	0.496542	0.008945	0.019826	0.005711
45° x 1.3	0.00000	0.00000	0.495091	0.008708	0.019019	0.006961
90° x 1.5	0.00000	0.00000	0.495644	0.008691	0.020185	0.006881

It is observed that Z.M orders 1 and 2 have null values and order 3 is significant. Thus only φ_3 *to* φ_6 are utilized to train the RBF classifier.

Radial Basis Function Parameter Initialization

In order to execute RBF neural network, only one parameter need to be initialized, namely spread. Spread is to control the width of *r* unit in the hidden layer. According to Table 6, the best spread value for Radial Basis Architecture is 0.01 because its sum square error (SSE) and computation time is the least from other spread values. Table 7, 8 and 9 shows the comparison for Goal Oriented Radial Basis Architecture, Generalized Regression Neural Network and Probability Neural Network respectively. It shows that the best spread value for three architectures in the training phase is 0.001 since it produces zero error and the computation time is the least as compared to other spread values.

Table 6: Comparison the best spread parameter value according SSE for Radial Basis Architecture

Neurons in Hidden layer	Goal	Spread	SSE	Computation Time
300	0.01	0.001	0.0118026	44.42
175	**0.01**	**0.01**	**0.0105504**	**15.84**
375	0.01	0.1	0.227323	150.77

Table 7: Comparison the best spread parameter value according computation time for Goal Oriented Radial Basis Architecture

Spread	Computation Time	Total Error
0.001	0.55	0
0.005	0.56	0
0.01	0.59	0
0.05	0.7	0
0.1	0.7	0
0.5	0.77	0.75
1	0.69	0
5	0.67	19.01

Table 8 : Comparison the best spread parameter value according computation time for Generalized Gaussian Neural Network Architecture

Spread	Computation Time	Total Error
0.001	0.09	0
0.005	0.13	0
0.01	0.09	11.48
0.05	0.11	15.22
0.1	0.13	36.92
0.5	0.13	42.86
1	0.06	43.8
5	0.13	38.69

Table 9 : Comparison the best spread parameter value according computation time for Probabilistic Neural Network Architecture

Spread	Computation Time	Total Error
0.001	0.19	0
0.005	0.13	0.7
0.01	0.13	6.35
0.05	0.08	40.3
0.1	0.09	39.02
0.5	0.13	45.16
1	0.14	39.02
5	0.13	43.31

Cross Validation Result

In order to verify that the network has generalized well, the sample data is divided into 4 sub sample. Since the total images are 390, 2 sub samples have 98 images while another two sub samples have 97 images. The network was trained and tested for four times. Three sub samples will act as the training data and one sub sample will be the test data. By using this approach, each sample will experience being in the test set and training set at dissimilar cycle. Figure 10 illustrates the sequence of data exchanges.

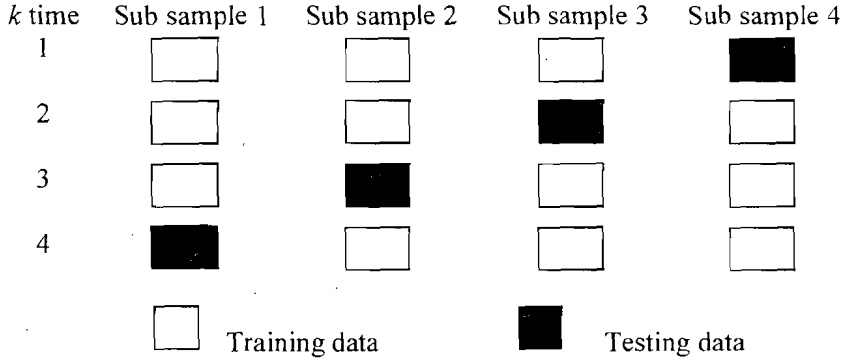

Figure 10: Sub sample representation for each *k* times

Table 10 illustrates the performance for the four RBF architecture evaluated. The spread for Radial Basis Architecture is different form others since with the value of 0.01, it produces the least sum square error (SSE) as indicated in Table 7. It is observed that the classification performance of Goal Oriented Radial Basis Architecture, Generalized Gaussian Neural Network Architecture and Probabilistic Neural Network Architecture is excellent, each of them achieve 100% accuracy. On the other hand, Radial Basis Architecture only achieves 97% accuracy.

Table 10: Classification Performance for Four RBF Architectures

Train	Spread	SSE	*k* cycle	time	NCC
rb	0.01	0.0105504	1	15.84	98
			2	15.5	97
			3	16.42	98
			4	16.14	97
			Mean time	15.98	100
gorb	0.001	-	1	0.55	98
			2	0.78	97
			3	0.56	98
			4	0.56	97
			Mean time	0.61	100
grnn	0.001	-	1	0.09	98
			2	0.22	97
			3	0.08	98
			4	0.11	97
			Mean time	0.13	100
pnn	0.001	-	1	0.19	98
			2	3.3	97
			3	0.13	98
			4	0.09	97
			Mean time	0.93	100

Legend;
In Table 10, **rb** represents Radial Basis Architecture
gorb represents Goal Oriented Radial Basis Architecture
grnn represents Generalized Gaussian Neural Network Architecture
pnn represents Probabilistic Neural Network Architecture

We focus now on the computation time aspect, it is observed that the Probabilistic Neural Network Architecture has the fastest speed, followed by Generalized Gaussian Neural Network Architecture then Goal Oriented Radial Basis Architecture. Conversely Radial Basis Architecture has the slowest computation time. The reason we examine the computation time is that, to explore the feasibility of adopting the classifier for large data set in a real-time application. Among the four architectures examined, Generalized Gaussian Neural Network Architecture not only exhibit perfect classification but also can be performed the task the fastest. This is due to the fact that the architecture has a function approximation capability. Here, weights are assigned and not "trained". Existing weights will never be alternated but only new data are inserted into weight matrices when training, thus making it a suitable candidate for real-time classification application.

6. CONCLUSION

In this work, we examined the performance of four RBF based architecture in classifying aircraft images. The images are represented using Zernike Invariant Moment that is invariance towards rotation and scaling. The architectures that are evaluated are Radial Basis Architecture, Goal Oriented Radial Basis Architecture, Generalized Gaussian Neural Network Architecture and Probabilistic Neural Network Architecture. Out of the four architectures explored, Generalized Gaussian Neural Network Architecture exhibits the perfect classification at the fastest time. This is due to its function approximation ability that does not repeatedly update the existing weights, only new data are inserted into weight matrices during training. Thus, we can claim that Generalized Gaussian Neural Network Architecture is suitable to be utilized for real-time image classification application.

REFERENCES

Abo-Zaid, A.M (1996). *A simple invariant neural network for 2-D image recognition* Radio Science Conference, 1996. NRSC apos;96., Thirteenth National, ISBN: 0-7803-3656-9, 19-21 Mar 1996, pp 251 – 258.

Botha E. C. (1994). *Classification of aerospace targets using superresolution ISAR images.* 0-7803-1998-2. pp 138-145.

Chun, J. H. *et al.* (2001). *Airport pavement distress image classification using moment invariant neural network. Asian conference on Remote Sensing.* (CRISP) (SISV) (AARS). Nov 2001.

Fatemi, H., Kleihorst, R., Corporaal, H.and Jonker, P. (2003) *Real time face recognition on a smart camera,*". Proceedings of ACIVS 2003 (Advanced Concepts for Intelligent Vision Systems), (Gent, Belgium), 2003.

Haykin, S.(1994) "Neural Networks – A Comprehensive Foundation." Toronto, Canada: Maxwell Macmillan.

McAulay, A., Coker, A. and Saruhan, K. (1991). *Effect of noise in moment invariant neural network aircraft classification. Proceedings og the IEEE 1991 National Aerospace and Electronic Conference, NAECON.* Vol. 2 pp743-749.

Mukundan, R., and Ramakrishnan, K. R. (1998). *Moment Function In Image Analysis.* Farrer Road, Singapore: World Scientific Publishing.

Puteh Saad(2003), Trademark Image Classification Approaches using Neural Network and Rough Set Theory, Ph.D. Thesis, Universiti Teknologi Malaysia.

Puteh Saad (2004), *Feature Extraction of Trademark Images using Geometric Invariant Moment and Zernike Moment – A Comparison*, Chiang Mai J. Sci; 31(3):217-222.

Shahrul Nizam Yaakob, Puteh Saad and Abu Hassan Abdullah, *Trademarks classification by Moment Invariant and FuzzyARTMAP*, Proc. of the Tenth Int. Symp. on Artificial Life and Robotics (AROB 10^{th} '05), 13^{th} – 14^{th} May 2005.

Shahrul Nizam Yaakob. *Classification of binary insect images using Fuzzy and Gaussian ARTMAP Neural Network* . MSc. Thesis. Kolej Universiti Kejuruteraan Utara Malaysia; 2006

Somaie, A. A., Badr, A. and Salah, T. (2001). *Aircraft image recognition using back-propagation. Radar, 2001 CIE International Conference on, Proceedings.* ISBN: 0-7803-7000-7, 2001.

Teague, M. R (1980). *Image analysis via the general theory of moments. Journal of the Optical Society of America.* Vol 70, No.8 pp920-930

www.airliners.net. (10 Ogos 2007)

Howard Demuth and Mark Beale, *Neural Network Toolbox for Use with MATLAB: User's Guide (v. 4)*, The Mathworks, Inc., 2001.

Appendices

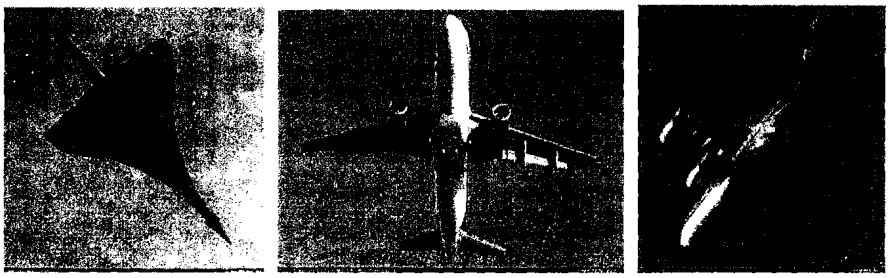

(a) (b) (c)

(d) (e)

(f) (g) (h)

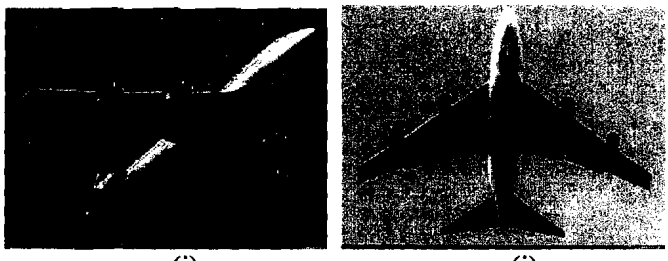

(i) (j)

Figure 6 : Category 1

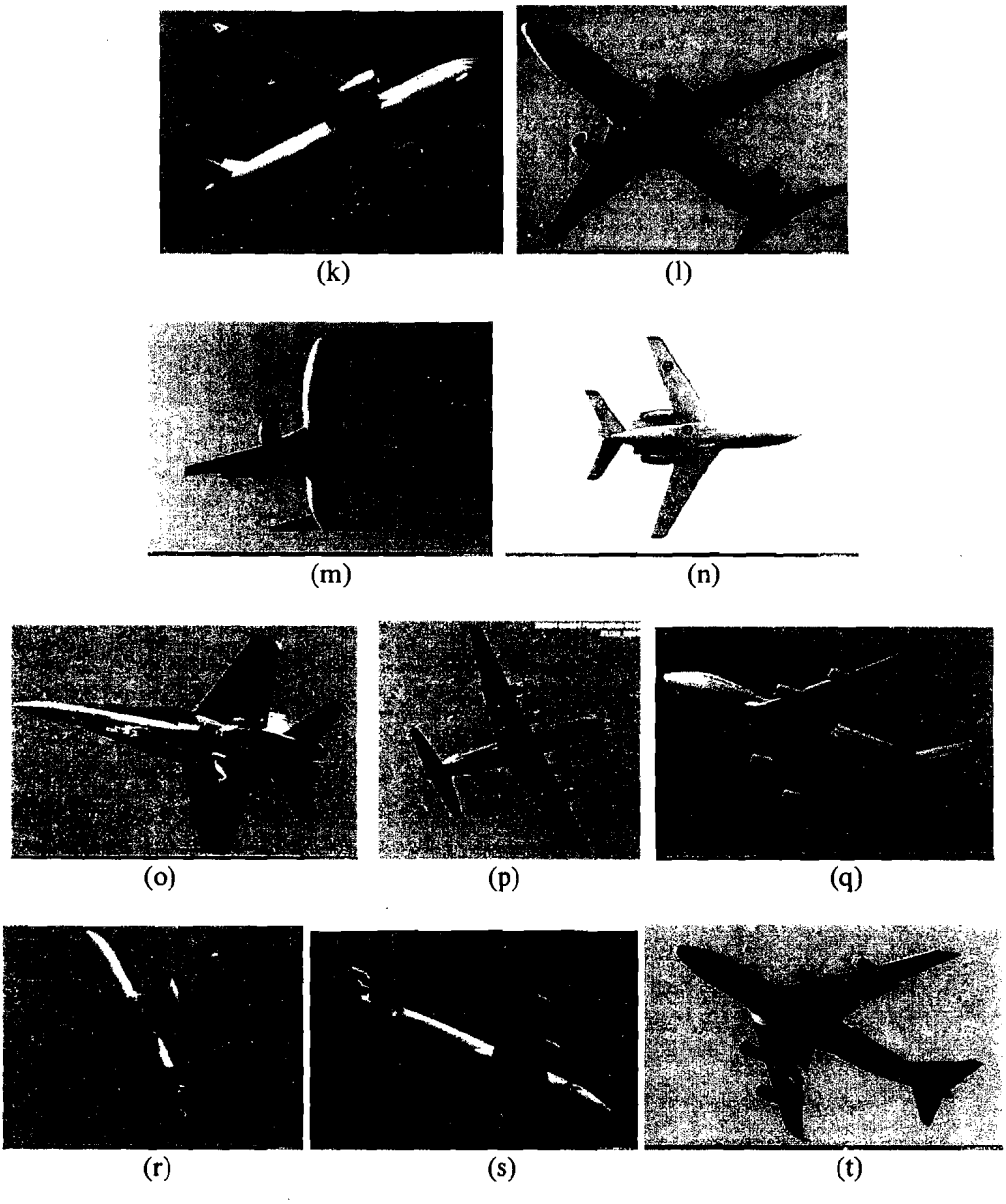

Figure 7 : Category 2

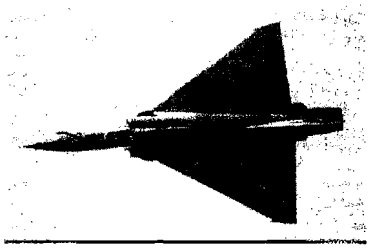

(u)

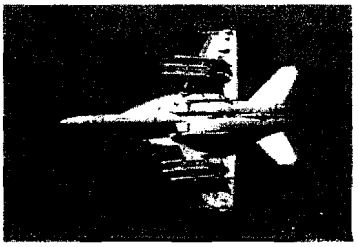

(v)

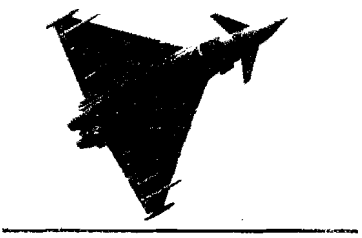

(w)

(x)

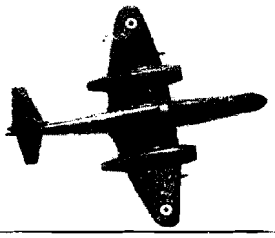

(y)

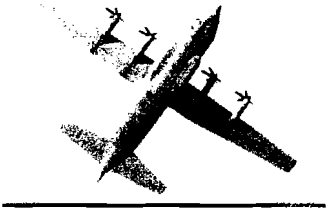

(z)

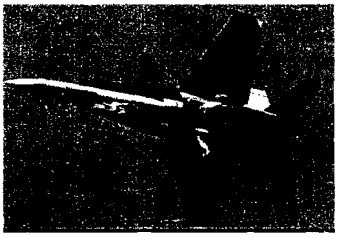

(z-1)

(z-2)

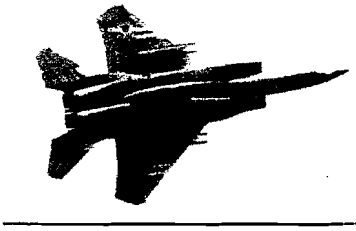

(z-3)

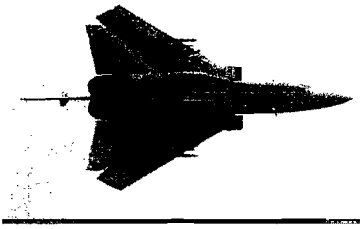

(z-4)

Figure 8 : Category 3

Table 1 : Category 1

Image	Image name
a	Aerospatiale-British Aerospace Concorde 102
b	Airbus A320-214
c	Airbus A340-313X
d	Airbus A320-232
e	Airbus A380-841
f	Boeing 747-4B5
g	Boeing 747-4J6M
h	Ilyushin Il-62M
i	Boeing 747-41R
j	Boeing 747SP-94

Table 2 : Category 2

Image	Image name
k	Airbus A330-243
l	Boeing 737-824
m	Boeing 737-...
n	Dassault Falcon 10
o	McDonnell Douglas MD-11
p	DC-6A N70BF
q	Boeing 747-4B5ERF
r	Boeing 767-238 ER
s	Boeing 747-245F SCD
t	Boeing 747-422

Table 3 : Category 3

Image	Image name
u	Boeing F SLASH A-18F Super Hornet
v	Dassault Mirage 2000C
w	Eurofighter EF-2000 Typhoon T1
y	Fairchild OA-10A Thunderbolt II
z	Gloster Meteor NF11
z-1	Lockheed Martin C-130J Hercules C5 (L-382)
z- 2	McDonnell Douglas F-18D Hornet
z- 3	McDonnell Douglas FA-18C Hornet
z-4	Mitsubishi F-15J Eagle
z-5	Panavia Tornado F3 (1)